Journal of Thermal Analysis, Vol. 35 (1989) 2143–2152

TG AND DSC STUDIES ON Sm(III) AND Tb(III) TARTRATES

R. M. Sharma and *M. L. Kaul*[+]

DEPARTMENT OF CHEMISTRY, UNIVERSITY OF JAMMU, JAMMU, 180004, INDIA

(Received March 24, 1988; in revised form March 27, 1989)

The tartrate monohydrates of Sm(III) and Tb(III), $Sm_2C_{12}H_{12}O_{18}\cdot H_2O$ and $Tb_2C_{12}H_{12}O_{18}\cdot H_2O$, were prepared and characterized on the basis of their elemental analysis and IR spectral studies. The thermal decompositions of these compounds, studied by TG and DSC methods, were found to follow an almost uniform pattern. Decomposition occurs in four steps. The first step involves dehydration, accompanied by partial decomposition to the oxalate, followed by conversion to the carbonate. The ultimate product in each case is the oxide M_2O_3, where M = Sm or Tb.

Reflectance spectra of the terbium compound were recorded at various stages of decomposition. The kinetics of the first decomposition step was studied by the non-isothermal method. TG and DSC data for this step were analysed for the evaluation of various kinetic parameters. Reasonable values of E, Z, and ΔS^+ were obtained. α *vs.* T curves were drawn on the basis of the TG and DSC data. The results suggest that the mechanism involves random nucleation.

Studies on the thermal decomposition and kinetics of thermal decomposition of the carboxylates of rare earth metals have attracted much interest in recent years [1–5] as, apart from providing an insight into the mechanism involved in the decomposition process, they can be used to establish the stability of these compounds and of the intermediates formed during their thermal decomposition. As a continuation of our earlier work on the thermal decomposition and kinetics of decomposition of tartrates of rare earth metals, we now report results on Sm(III) and Tb(III) tartrates.

Experimental

$Sm_2C_{12}H_{12}O_{18}\cdot H_2O$ and $Tb_2C_{12}H_{12}O_{18}\cdot H_2O$ were prepared in the same manner as the tartrates of Nd(III) and Gd(III) reported earlier [6]. The percentage of the metal was estimated gravimetrically by precipitating it as $M(OH)_3$ and weighing as M_2O_3, and those of carbon and hydrogen by microanalysis.

John Wiley & Sons, Limited, Chichester
Akadémiai Kiadó, Budapest

A Shimadzu IR–435 spectrophotometer (Japan) was used to obtain the infrared spectra, via KBr pellets, in the range 4000–400 cm^{-1}.

A Mettler TA–3000 system (Switzerland) was used to record simultaneous TG and DTG curves up to 1173 K in static air and DSC curves up to 823 K in nitrogen atmosphere at a heating rate of 10 deg min^{-1}.

The values of α, the fractional weight loss at different temperatures, were computed from the TG curves and α *vs.* T plots were produced. Such plots were also drawn from the DSC data by taking α as a/A, where a is the area of the DSC peak up to a particular temperature and A is the total area of the peak. The kinetics of the first decomposition step was investigated by a non-isothermal method, using TG and DSC data and applying appropriate kinetic equations.

The reflectance spectra of samples of the terbium compound, taken as a typical case, preheated to desired temperatures as indicated by the TG curve, were recorded (360–210 nm) on a Beckman–DK–2A reflectance spectrophotometer, the concentration being the same in every case, with MgO as reference material (speed = 36 nm/min, scale = 10 nm/cm and sensitivity = 20).

Results and discussion

(a) Samarium tartrate

The elemental analysis of the compound gave Sm, 40.32; C, 18.70; H, 1.50% ($Sm_2C_{12}H_{12}O_{18} \cdot H_2O$ requires: Sm, 39.37; C, 18.89; H, 1.84%).

The IR spectrum of the compound shows a strong and broad band at 3400 cm^{-1} due to O—H stretching vibrations of water and secondary alcohol groups. $\nu_{asym(OCO)}$ and $\nu_{sym(OCO)}$ bands appear at 1600 cm^{-1} and 1365 cm^{-1}, respectively. A doublet at 1110 cm^{-1} suggests that the two C—OH groups are co-ordinated dissimilarly, as in the case of other corresponding compounds [6, 7].

The thermal decomposition of samarium tartrate monohydrate occurs in four steps. Figure 1 shows the TG–DTG curves with the superimposed DSC curve of the compound. The DTG and DSC peaks for the various decomposition steps correspond to the changes indicated by the TG curve.

The first step of decomposition starts near 320 K and extends up to 510 K. The decomposition is prolonged to 543 K in nitrogen atmosphere in which a DSC study was carried out. Such delayed decomposition in nitrogen atmosphere has also been reported for similar compounds [8]. The observed and calculated losses in weight during this step correspond to dehydration of the compound, with simultaneous partial conversion to the corresponding oxalate, $Sm_2C_{12}H_{12}O_{18} \cdot Sm_2(C_2O_4)_3$. This intermediate remains stable up to 534 K, as indicated by the arrest in the TG curve from 510 K to 534 K.

The second decomposition step starts near 540 K and continues up to 648 K. The extent of weight loss at the end of this step suggests the formation of $Sm_2C_{12}H_{12}O_{18} \cdot Sm_2(CO_3)_3$. The slackening of the TG curve between 648 and 658 K suggests that this intermediate remains as such within this range of temperature.

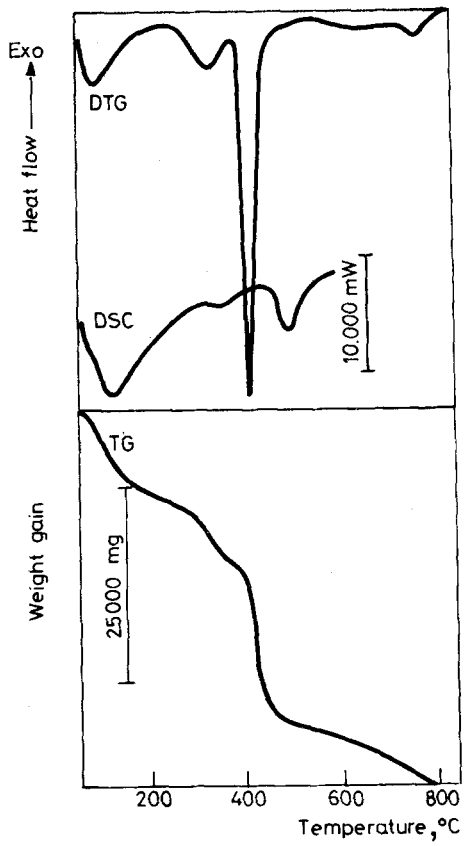

Fig. 1 TG–DTG curves (sample wt. = 9.235 mg) with superimposed DSC curve (sample wt. = 8.490 mg) of samarium tartrate

The third step commences beyond 658 K and proceeds up to 793 K. The total weight loss at this temperature indicates the formation of $Sm_2(CO_3)_3 \cdot Sm_2O_3$. This remains stable up to 832 K.

The fourth step starts beyond 832 K and is marked by a comparatively slower loss in weight until samarium oxide, Sm_2O_3, is formed as the end-product. This remains stable beyond 1058 K, as no further loss in weight occurs on subsequent heating of the compound.

The DSC curve shows two broad endothermic regions at 313–543 K and 548–648 K, with peak maxima at 393 K and 583 K. Another endothermic region appears at 663–793 K, having peak temperature at 724 K.

The IR spectrum of the compound heated to 520 K shows all the characteristic bands of the original compound, except that the band at 3400 cm^{-1} appears with an appreciable decrease in intensity, suggesting the elimination of a water molecule and thus indicating the formation of a different intermediate up to this temperature.

(b) Terbium tartrate

The compound on analysis gave Tb, 40.48; C, 18.40; H, 2.10% ($Tb_2C_{12}H_{12}O_{18} \cdot H_2O$ requires: Tb, 40.75; C, 18.46; H, 1.79%).

The important absorption frequencies [6, 7] in the IR spectrum of the compound appear at 3380 (s, b) cm^{-1}, 1585 cm^{-1}, 1375 cm^{-1} and 1100 cm^{-1} (doublet), due to the O—H stretch of water and secondary alcohol groups, $\nu_{asym(OCO)}$, $\nu_{sym(OCO)}$ and two dissimilar C—OH groups, respectively.

The decomposition of the compound occurs in four stages. The first stage starts from 320 K and continues up to 497 K. However, in nitrogen atmosphere it starts at lower temperature (313 K) and is delayed up to 513 K. The weight loss during this stage indicates the removal of a water molecule, together with simultaneous partial conversion into the oxalate, $Tb_2C_{12}H_{12}O_{18} \cdot Tb_2(C_2O_4)_3$. This intermediate remains stable up to 525 K, as indicated by the horizontal portion of the TG curve between 497 and 525 K.

The second stage of decomposition starts above 525 K and a regular loss in weight occurs up to 657 K. The loss in weight during this step corresponds to the formation of $Tb_2C_{12}H_{12}O_{18} \cdot Tb_2(CO_3)_3$, which remains stable from 657 K to 670 K, as shown by a small arrest in the TG curve.

The third decomposition stage starts beyond 670 K and continues with a regular loss in weight up to 761 K. The intermediate formed in this stage corresponds to $Tb_2O_2CO_3$. The formation of such compounds has already been reported in the decomposition of some other salts of rare earth metals [8, 9]. The intermediate formed in this step remains stable from 761 K to 777 K.

The forth stage of decomposition is observed from 777 K to 1076 K. The weight loss at the end of this step corresponds to the formation of terbium oxide, Tb_2O_3, as the final product.

The DSC curve reflects the changes seen in the TG curve. It shows three endothermic regions, at 313–513 K, 533–663 K and 668–813 K, with peak temperatures at 398 K, 572 K and 753 K, respectively.

From the reflectance spectra of the compound (Fig. 2) recorded at room temperature (318 K) and its samples preheated to different temperatures before and

soon after the completion of the first stage (indicated by TG), it is observed that the spectra at 373 K, 458 K and 503 K show a marked variation in the intensity of the bands near 300 nm. The absorptions near 260 nm and 230 nm also show variation as dehydration progresses with the rise of temperature. These bands are characteristic of the hydrates giving reflectance in the UV region. As dehydration sets in with the progressive increase of temperature, the reflectance (R_α) decreases and hence the absorbance $\log\left[\frac{1}{R_\alpha}\right]$ increases.

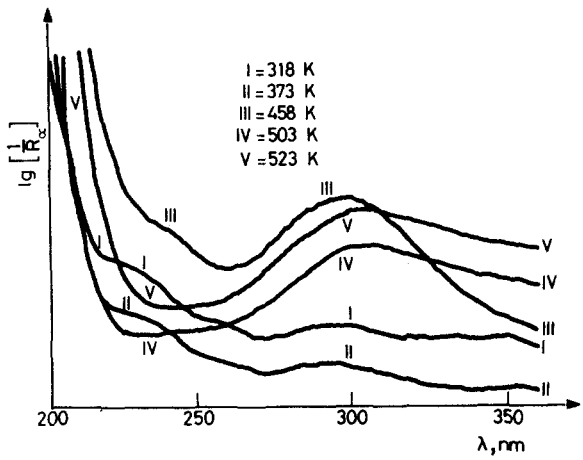

Fig. 2 Reflectance spectra of terbium tartrate

Kinetics of decomposition

The α *vs.* T curves of the two compounds, constructed on the basis of the TG and DSC data, display essentially the same pattern. The curves begin with an acceleratory period without any apparent induction period, and indicate that no surface nucleation or branching occurs before dehydration starts [10].

The kinetics of the first decomposition step for the two compounds was studied by the non-isothermal method, using both TG and DSC data. For the TG data, the equations used were:

1. Coats–Redfern equation [11]:

a) $$\log\frac{g(\alpha)}{T^2} = \log\left[\frac{-\ln(1-\alpha)}{T^2}\right] = \log\left[\frac{ZR}{\beta E}\left(1-\frac{2RT}{E}\right)\right] - \frac{E}{2.303RT}$$

(for $n=1$)

b) $$\log \frac{g(\alpha)}{T^2} = \log\left[\frac{(1-\alpha)^{1-n}}{\frac{1-n}{T^2}}\right] = \log\left[\frac{ZR}{\beta E}\left(1-\frac{2RT}{E}\right)\right] - \frac{E}{2.303RT} \quad (\text{for } n \neq 1)$$

2. Piloyan–Novikova equation [12]:

$$\log \frac{g(\alpha)}{T^2} = \log \frac{\alpha}{T^2} = \log \frac{ZR}{\beta E} - \frac{E}{2.303RT}$$

3. Horowitz–Metzger equation [13]:

a) $$\log g(\alpha) = \log[-\ln(1-\alpha)] = \frac{E\theta}{2.303RT_m^2} \quad (\text{for } n = 1)$$

b) $$\log g(\alpha) = \log\left[\frac{1-(1-\alpha)^{1-n}}{1-n}\right] = \frac{E\theta}{2.303RT_m^2} \quad (\text{for } n \neq 1)$$

where T = temperature, Z = pre-exponential factor, R = molar gas constant, β = rate of heating, E = energy of activation, T_m = peak temperature, $\theta = T - T_m$, $g(\alpha) = \int_0^\alpha \frac{d\alpha}{f(\alpha)}$ and $f(\alpha)$ is the appropriate function, depending upon the mechanism involved. Thus, $g(\alpha)$ values corresponding to different reaction models were calculated and the values of $\log \frac{g(\alpha)}{T^2}$ *vs.* T^{-1} were plotted for the Coats–Redfern and Piloyan–Novikova equations. The linear fits for various models were investigated in the former case, and that $g(\alpha)$ was chosen to decide the reaction mechanism and to arrive at the kinetic parameters which yielded the best fitting straight line. For both equations, E was calculated from the slope and Z from the intercept of such plots (Fig. 3). For the Horowitz–Metzger equation, plots of $\log g(\alpha)$ *vs.* θ were drawn and the best linear plot (Fig. 4) was chosen to find the appropriate $g(\alpha)$, and hence the correct mechanism. E was calculated from the slope of this plot. The following equation was used to calculate Z:

$$Z = \frac{E}{RT_m^2}\beta \exp\left(\frac{E}{RT_m}\right)$$

The entropy of activation (ΔS^*) was obtained from the equation

$$Z = \frac{kT_m}{h}\exp(\Delta S^*/R)$$

where Z is the Boltzmann constant and h is Planck's constant.

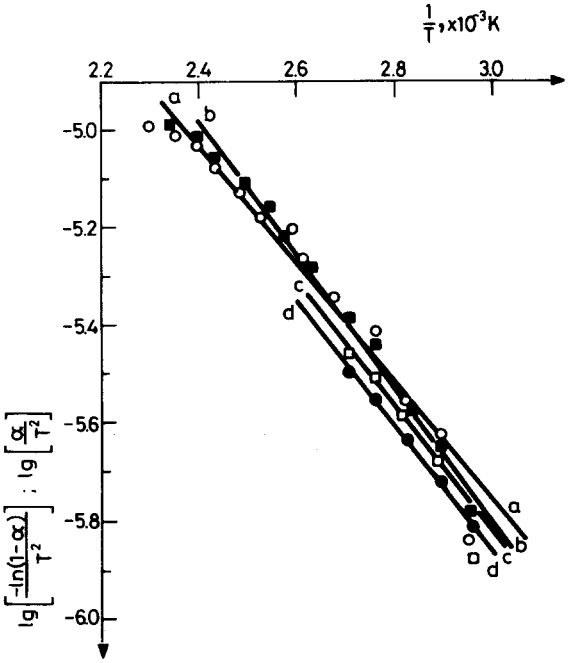

Fig. 3 Coats–Redfern plots: (a) samarium tartrate; (b) terbium tartrate. Piloyan–Novikova plots: (c) samarium tartrate; (d) terbium tartrate

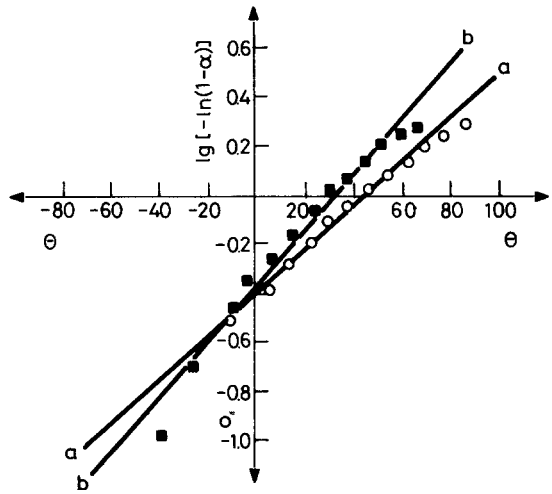

Fig. 4 Horowitz–Metzger plots: (a) samarium tartrate; (b) terbium tartrate

The following DSC methods were used for the determination of kinetic parameters:

1. The Roger–Morris–Smith method [14, 15]

The distances between the DSC curve and the base line at corresponding temperatures (K) from the onset to the maximum of the curve were measured. The logarithms of these distances were plotted *vs.* T^{-1}. The best straight line portion of the plot was selected for analysis (Fig. 5). If d_1 and d_2 are the distances at the

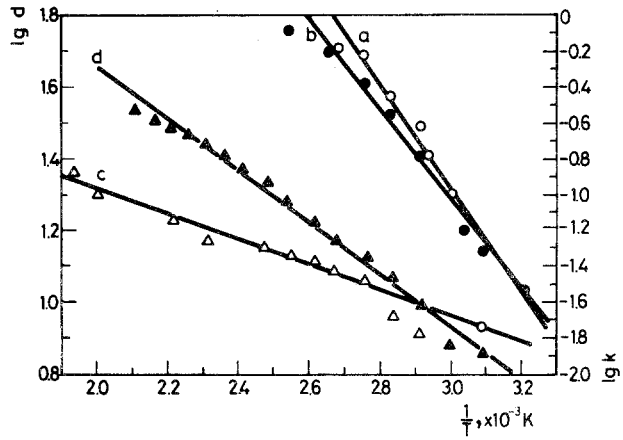

Fig. 5 Roger–Morris–Smith plots: (a) samarium tartrate; (b) terbium tartrate. Barrett plots: (c) samarium tartrate; (d) terbium tartrate

extremes of the selected linear portion corresponding to T_1^{-1} and T_2^{-1}, E was calculated by using the equation

$$-E = \frac{4.58 \log (d_1/d_2)}{T_1^{-1} - T_2^{-1}}$$

2. The Ellerstein method [16, 17]

Evaluation was made, by using the log form of the rate law:

$$\ln \frac{dH/dt}{\Delta H_{\text{total}}} = \ln A - \ln \beta - \frac{E}{RT} + n \ln \frac{\Delta H_r}{\Delta H_{\text{total}}}$$

where dH/dt is the instantaneous enthalpy change with respect to absolute temperature, ΔH_{total} is the total enthalpy under the peak, ΔH_r is the remaining part of the enthalpy at a given temperature and n is the apparent order of reaction. The enthalpy values ΔH_{total} and ΔH_r are proportional to the respective areas in the DSC curve.

3. The Barrett method [18]

E was obtained from the slope and Z from the intercept of the linear plot of $\log k$ *vs.* T^{-1} (Fig. 6) for various values of a and A, where $k = \frac{dH/dt}{A-a}$, and dH/dt is the height of the curve at a given temperature.

Table 1

Method	$Sm_2C_{12}H_{12}O_{18}\cdot H_2O$			$Tb_2C_{12}H_{12}O_{18}\cdot H_2O$		
	E, kJ mol^{-1}	Z, s^{-1}	ΔS^*, JK^{-1} mol^{-1}	E, kJ mol^{-1}	Z, s^{-1}	ΔS^*, JK^{-1} mol^{-1}
TG methods						
1 Coats–Redfern	25.48	6.4×10^{1}	−230.79	24.71	4.8×10^{1}	−233.53
2 Piloyan–Novikova	39.44	1.3×10^{3}	−186.88	32.68	9.9×10^{1}	−208.37
3 Horowitz–Metzger	23.38	1.3×10^{1}	−225.03	25.00	1.5×10^{1}	−224.05
DSC methods						
1 Barrett	22.98	1.5×10^{1}	−224.26	28.72	6.3×10^{2}	−193.72
2 Ellerstein	28.58	1.2×10^{5}	—	31.59	3.9×10^{5}	—
3 Roger–Morris–Smith	23.00	—	—	33.38	—	—

Table 1 presents the results obtained for the kinetic parameters.

It is found that for both compounds the best linear fit is obtained for $g(\alpha) = -\ln(1-\alpha)$ or $n=1$ in the application of methods based on TG. Thus, the first step of decomposition of samarium tartrate monohydrate or terbium tartrate monohydrate involves a random nucleation mechanism [19]. The DSC studies point to the same value of n and hence the same mechanism. The obtained values of the kinetic parameters are reasonable and in good agreement.

* * *

One of us (R.M.S.) is grateful to the U.G.C., New Delhi, for the award of a teaching fellowship.

References

1 S. Sampath and D. M. Chackraburtty, India A.E.C. Bhaba; 6 PP (1972) 631.
2 A. I. Turova and V. V. Serebrennikov, Tr. Tomsk Univ., 240 (1973) 138 (In Russian).
3 L. N. Bindarava, R. M. Dvornika and L. A. Gutru, Zh. Neorg. Khim. No. 19, issue 10 (1974) 2659 (in Russian).
4 M. L. Kaul, K. K. Raina and P. N. Kotru, J. Mater. Sci., 21 (1986) 3933.

5 M. L. Kaul, K. K. Raina and P. N. Kotru, Ind. J. Pure and Appl. Physics, 25 (1987) 224.
6 R. M. Sharma and M. L. Kaul, J. Indian Chem. Soc., 64 (1987) 459.
7 K. C. Satpathy and P. Herna, J. Indian Chem. Soc., 58 (1981) 1002.
8 A. I. Turova, I. A. Shynpand and V. V. Serebrennikov, Tr. Tomsk. Gos. Univ., 237 (1973) 27 (in Russian).
9 W. Brzyska and W. Ferene, J. Thermal Anal., 22(1) (1981) 53.
10 D. A. Young, The International Encyclopaedia of Physical Chemistry, Solid and Surface Kinetics, F. C. Tompkins, Pergamon Press, London, 1966, p. 5.
11 A. W. Coats and J. P. Redfern, Nature, 201 (1964) 68.
12 G. O. Piloyan, I. S. Novikova and I. D. Ryabehik, Nature, 212 (1966) 1229.
13 H. Horowitz and G. Metzger, Anal. Chem., 35 (1964) 1464.
14 R. N. Roger and E. D. Morris, Anal. Chem., 38 (1966) 412.
15 R. N. Roger and L. C. Smith, Anal. Chem., 39 (1967) 1024.
16 S. M. Ellerstein, J. Phys. Chem., 69 (1965) 2471.
17 S. M. Ellerstein, Analytical Calorimetry, Vol. 2, R. S. Porter & J. F. Johnson, Plenum Press, New York, 1970, p. 391.
18 K. E. J. Barrett, J. Appl. Polymer Sci., 11 (1967) 1617.
19 K. L. Mampal, Z. Physik Chem., 187(A), (1940) 43, 235.

Zusammenfassung — Die Tartratmonohydrate von Sm(III) und Tb(III), $Sm_2C_{12}H_{12}O_{18} \cdot H_2O$ und $Tb_2C_{12}H_{12}O_{18} \cdot H_2O$ wurden hergestellt und mittels Elementaranalyse und IR-Spektren charakterisiert. Die thermische Zersetzung dieser Verbindungen wurd mittels TG und DSC untersucht und als fast gleichmäßig verlaufend befunden. Die Zersetzung erfolgt in vier Schritten. Der erste Schritt besteht in der Dehydratierung, begleitet von einem teilweisen Zerfall in die Oxalate und gefolgt von einer Bildung der Karbonate. Das Endprodukt ist in allen Fällen das Oxid M_2O_3 mit M = Sm oder Tb. Bei mehreren Stufen des Zerfalles der Therbiumverbindung wurden Reflexionsspektren aufgenommen. Die Reaktionskinetik des ersten Reaktionsschrittes wurde mit der nichtisothermen Methode untersucht. Zur Ermittlung verschiedener kinetischer Parameter wurden die TG- und DSC-Daten für diesen Schritt ausgewertet. Für E, Z und ΔS^* konnten akzeptable Werte erhalten werden. Auf der Grundlage der TG- und DSC-Daten wurden außerdem $\alpha - T$-Diagramme erstellt. Die Resultate zeigen, daß der Reaktionsmechanismus Random-Keimbildung beinhaltet.

Резюме — Получены и охарактеризованы элементным анализом и ИК спектрами моногидраты тартратов трехвалентных самария и тербия общей формулы $M_2C_{12}H_{12}O_{18} \cdot H_2O$. Изученное методами ТГ и ДТГ термическое разложение этих солей показало их идентичный характер. Реакция разложения протекает в четыре стадии. Первая стадия включает дегидратацию, сопровождающуюся частичным разложением их до оксалатов с последующим превращением до карбонатов. Для обоих солей конечным продуктом разложения являлся оксид металла. Для соли тербия измерены спектры отражения на различных стадиях ее разложения. Неизотермическим методом изучена кинетика первой стадии разложения. Данные ТГ и ДТГ измерений первой стадии разложения были использованы для оценки различных кинетических параметров. Получены приемлемые значения E, Z и ΔS^*. На основе данных ТГ и ДТГ выведены кривые в координатах $\alpha - T$. Результаты исследования предполагают механизм реакции произвольного образования центров кристаллизации.